

EVALUATION OF AN ADDITIVELY MANUFACTURED TOOLING WITH INTEGRATED FUNCTIONALITY FOR THE PRODUCTION OF CARBON FIBER TEXTILE PREFORMS

Deden, Dominik. Buchheim, Andreas. Stefani, Thomas.

German Aerospace Center

Institute of Structures and Design – Center for Lightweight Production Technology

Am Technologiezentrum 4

86159 Augsburg, Germany

ABSTRACT

The recent progress in additive manufacturing technologies has led to new freedom in respect to part design. Strongly undercut and inner geometries can be manufactured as an integral structure. In the course of the development of an automated preforming process for small batch freeform CFRP components at the German Aerospace Center in Augsburg, the possibility of additive manufacturing for preform toolings was assessed. A segmented preform tooling made from polyamide 12 enriched with aluminum powder was manufactured in a selective laser sintering (SLS) process. Apart from the formative geometry additional functions were integrated in the design, such as pneumatic fixation of plies, heating, cooling as well as the integration of sensors for the monitoring of process parameters. The results of the automated preforming process are generally favorable. However, inherent disadvantages of additive manufacturing, like thermal warpage, need to be considered in order to determine the suitability of the tooling for the preforming process. Therefore, an analysis of geometric variance and performance of the integrated functions is done. The results are critically examined against the background of the preforming process and used to discuss opportunities and limitations of additively manufactured toolings for the general application in production of preforms.

1. INTRODUCTION

The production of toolings for complex CFRP parts is expensive and time consuming with the use of subtractive manufacturing techniques. Further geometries like die-cuts cannot be manufactured in one piece. With the ongoing improvement in additive manufacturing (AM) the quality of the final contour of parts has progressively increased. The production of molds made in an additive process is called rapid tooling. Preforming of textiles for the production of CFRPs poses an interesting use-case for rapid tooling. That is because preforming is an early step during production of CFRP parts. Therefore the final surface of the part is defined later during infusion and curing of the part and the impact of geometric inaccuracies on the finished part is minimal. Further the freedom of design offered by AM enables the integration of additional functionality in the design of the tooling. Examples for useful functions are the fixation of plies during the draping of the textiles or during the transport of the sub-preforms in an automated process, the heating of the molds for binder activation and active cooling of the activated preform. In our use case of an automated production, the final preform consists of four sub-preforms that are subsequently assembled and cured in a resin transfer molding (RTM) process using another

formative tool. For an automated production the separation of process steps creates the need for additional toolings. If the preforming is isolated from the curing process, rapid tooling is an inexpensive alternative to subtractive manufacturing of molds. This paper deals with the feasibility of rapid tooling for preforming using the example of two molds manufactured in a selective laser sintering (SLS) process.

2. STATE OF THE ART

The following gives an overview of related work that has been done in the past. The information is useful for the understanding of the context of this work.

2.1 Rapid Tooling

Rapid tooling is a generic term that describes the fast manufacturing of molds, usually in an additive manufacturing process. The material and type of process is not further specified. Usually a lower accuracy is accepted for the sake of time reduction and cost savings. The application rapid tooling is most commonly used in is the development of metal toolings for injection molding. Major advantages of rapid tooling for injection molding is the integration of cooling channels for higher cycle times and the decreased development costs for toolings that often need iterations before the final design [1]. Another big field of application is the production of complex cast molds and sand cores for casting. In recent years rapid tooling has become more common in the realm of composites as well. There are efforts to use 3D printed molds from short fiber reinforced materials for industrial autoclave processes [2]. Further additively manufactured sacrificial cores that are strong enough for autoclave curing and can be washed out have been developed for CFRP production by Stratasys [3]. Another application of rapid prototyping for FRP found in literature is the use of additively manufactured inserts for a pressing tool made from metal in a selective laser melting process. The inserts were used for the pressing of sheet molding composite [4]. Contrary to these applications for preimpregnated fibers there are few examples of dry fiber processes using rapid tooling. A study focusing on printed molds for hand-layup found that cost effective plastic molds can only be used in production for a very limited number of times. The fast degradation of the molds surface is caused by the epoxy. However compared to the cost of traditional toolings made from metal the approach is still economical [5].

2.2 Molds for Preforming

In the industrial production of components made of fiber reinforced plastics a range of mold materials can be used depending on the application. Normally metallic molds are used because of their easy availability, machinability and reparability. Additional benefits result from high accuracy requirements and the extended tool life with regard to the abrasive carbon fibers. Also their surface is resistant to solvent and release agents. Within the metallic materials steel S235 JR or aluminum AlMg3 are comparable inexpensive and therefore widely used. For processes requiring consolidation and resin curing in an oven or autoclave, mostly high-alloy steels e.g. INVAR36 are used to minimize the thermal expansion coefficient deviations of carbon and metal in order to obtain dimensionally stable components. Despite the difference in thermal expansion another disadvantageous is the high weight which makes the handling especially for larger sized parts more difficult and the high thermal mass impedes an even temperature distribution.

For smaller quantities, lower accuracy requirements or special applications tool molds made of CFRPs are used. Compared to the metal molds they are lower priced in production and have lower weight. However, the manufacturing process requires a prototype model of which the component geometry is mapped. Disadvantages compared to metallic molds are the shorter tool life due to the degradation of the plastic surface, the reduced level of temperature resistance and the lower dimensional accuracy due to distortion during production. The identical coefficients of thermal expansion between component and mold shape are advantageous [6].

Polyurethanes (PUR) are often used for experimental applications and initial tests. The material is mechanically easy to work and has low material costs. Disadvantages are the limited operating temperature and the low toughness of the material.

3. CONCEPTION

The toolings considered in this work were originally designed for an automated preforming process for complex spherical components of small to medium size. The final preform consists of four sub-preforms that are applied to a foam core after draping. The method of draping chosen for the process requires a male geometry that matches the female mold [7]. In the following chapter general requirements for molds in preforming processes are presented and specific requirements for the use case are defined. Subsequently the resulting design and method of production are discussed.

3.1 Requirements and Definitions

In general preform toolings need to be formative to the final geometry of the part within a certain allowance. In the given use case the parts are not cured in the same tooling as they are draped in. Deviations in the surface geometry and the roughness of the surface will therefore not show in the cured part. However the accuracy of the surface must be high enough to ensure a match between the male drape tool and the female tooling. Further a smooth surface is required so the textiles stay intact during draping. Usually the molds need to be temperature stable, since heat is required either during curing or for the activation of the epoxy binder. The binder used is Hexcel E01 powder. The operating temperature for activation is 80 °C to 140 °C with a dwell time of 15 minutes. To ensure a consistent activation of the preform the temperature difference over the surface cannot exceed 30 °C [8]. The choice of material for the tooling is further restricted by chemical compatibility. At the one hand contact between the fibers and certain materials like uncured silicon are not allowed. On the other hand the thermal activation of the epoxy binder makes the use of an adhesive necessary to demold the preform. Apart from the physical and chemical demands regarding the material there are requirements for the producibility of the molds and their application in the use case. After researching possible materials and AM processes we found, that a SLS process provides the necessary accuracy as well as a range of materials that have a melting point above our operating temperature. One option for SLS that also has inherent adhesive qualities is polyamide 12 (PA12). We concluded to use a PA12 enriched with aluminum powder called Alumide. Selective mechanical and thermal properties of Alumide compared to an average PA12 material are shown in Table 1.

Table 1: Comparison of selected properties of PA12 and PA12 enriched with Aluminum (Alumide) [9]

	Polyamide 12 (PA2202)	Alumide
Density [Kg/m ³]	980	1360
Melting Temp. [°C]	176	176
Temp. of deflection under Load [°C]		
1.80 MPa	75	144
0.45 MPa	154	175
Young's Modulus [MPa]	1850	3800
Shore D hardness (15s)	75	76

Although not quantified by the manufacturer, the heat conductivity of the alumide is expected to be increased in comparison to the PA12 due to the 23.4 % content of aluminum. The melting temperature is unaffected by the aluminum. Although the melting point is above the operation temperature of the toolings, melting due to heat accumulation inside the tooling is a risk. Therefore we chose self-limiting heating cables as a heat source, normally used for electric trace heating. Depending on the temperature of the cable, the power is limited. The maximum temperature of the cables used for the molds is 120 °C. A possible problem resulting from self-limiting heating cables is that the maximum temperature inside the cable is exceeded before the surface of the mold reaches its operating temperature resulting in an uneven heat distribution over the surface.

3.2 Design and Production

As mentioned before the preform of the use case is quadripartite. The complete mold consists of two large-area toolings and two toolings for the edges. Since each pair is designed similarly, only one tooling of each pair will be discussed as an example. The functions that were integrated into all four designs are channels for the self-limiting heating cables, a network of channels for pneumatic manipulation and small channels that end in defined positions underneath the tooling surface for near-surface sensor placement. Further three reference points for the alignment of the mold during the automated process are placed on the surface. Figure 1 shows the CAD-model of the large-area tooling. The inner geometry is highlighted in blue.

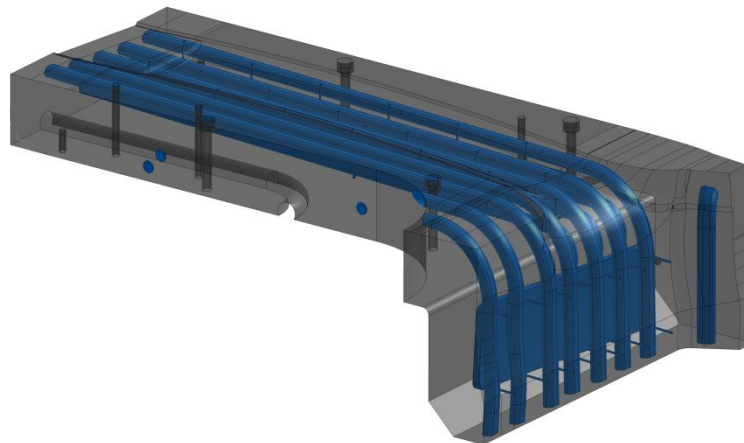


Figure 1: Large-area tooling with highlighted inner geometry (blue)

There are eight channels for the heating cables which are designed to be roughly 3 mm beneath the surface. The exact distance may vary in order to straighten the channels. This is necessary due to the rigidity of the heating cables. The cables are 27 mm apart from each other. The distance is necessary to leave room for the air channels that connect the surface orifices with main air chamber that lies underneath the heating channels. The orifices have a diameter of 1.5 mm. The grid of the orifices on the surface is roughly 27 mm by 56 mm. The tooling has maximum outer dimensions of 140 mm × 470 mm × 250 mm.

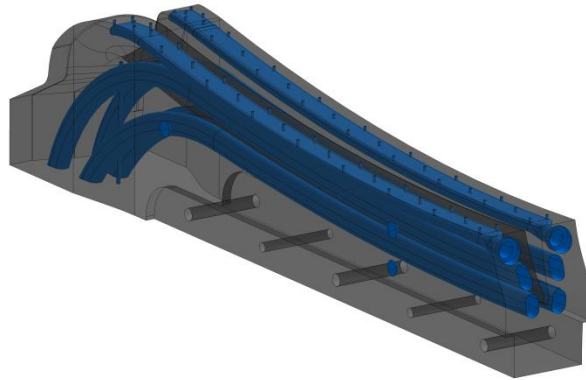


Figure 2: Edge tooling with highlighted inner geometry (blue)

The edge tooling depicted in Figure 2 has a total of four channels for the heating cable. Due to the shape of the functional surface the channels had to be tilted in order to bring in the heat close to the surface. Due to the limited flexibility of the heating cables across their horizontal axis a consistent distance to the surface was not achieved. As a tradeoff the cables have a close distance of 3 mm in the most relevant part for the activation of the binder. One major difference to the large-area tooling is the placement of the orifices for fixation. Since there is no need for fixation in the area of the edge, the textiles need to be held in place before the draping. Therefore the orifices are placed in a non-formative area of the mold. The tooling has maximum outer dimensions of 100 mm × 420 mm × 80 mm.

In order to reduce the risk of warping during production the toolings were designed to reduce material accumulations. Further not all the material was molten by the laser. The final molds are therefore thin-walled with a wall thickness of 5 mm, filled with the remaining unsintered powder of the SLS process. This way, less energy is brought into the part, the cooldown-time of the finished part is reduced and warping is minimized. The build direction was not specified for production.

4. EXPERIMENTAL SETUP AND RESULTS

Apart from the utilization of the molds in an experimental setup for automated preforming, the functionality of the additively manufactured molds was assessed in a series test. These tests were conducted to validate the geometry of the printed molds as well as the functionality of the integrated features.

4.1 Geometrical variance

The production of the molds was realized in a SLS process on an EOS P395 machine. As mentioned before the geometric accuracy is not crucial compared to a mold used for infusion and

curing. With regard to the draping of the fibers and the resulting fiber orientation a significant variance in shape is not tolerable. Due to the geometry of the designed toolings the SLS process had an inherent risk of warpage. For this reason a comparison between the CAD-geometry and the finished molds was conducted.

4.1.1 Methodology

In order to evaluate the geometric variance the finished parts were scanned using a dynamic Laser Scanner T-Scan 5 and the absolute Tracker AT960 both by Leica. The T-Scan measures the surface of the molds and generates a point cloud. The density of points for the measurement was at least 4.75 points per mm². Multiple scans were necessary to capture the molds. Therefore the density of point varies in the overlapping area of two scans. There have been two measurements per form – one right after production of the parts and a second after ten heating cycles. Further the molds have been used in the experimental setup they were designed for in between measurements. The generated point clouds were processed with the software Spatial Analyzer and exported to CATIA V5R23. In order to match the measured point cloud to the Surface, the three reference points on the mold were taken in the same position as the point cloud. Using the three reference points of the point cloud and the CAD-design of the mold two coordinate systems were created. Finally the coordinate systems were matched in CATIA and a distance analysis between the point cloud and the surface of the mold was done.

4.1.2 Results

After production the molds showed no major defects. The channels for the sensor placement inside of the tooling were still blocked by unsintered material. The distance analysis for the large-area tooling shows that 71% of the scanned points have a deviation of less than 0.3 mm and 97% a deviation of less than 0.75 mm in the normal direction of the surface. Major warping was not detected by the results. However shrinkage along the long side of the tooling is distinct. At the top side of the mold the length has shrunk by 0.24 mm relative to the center reference point. Figure 3 shows the distance analysis after production.

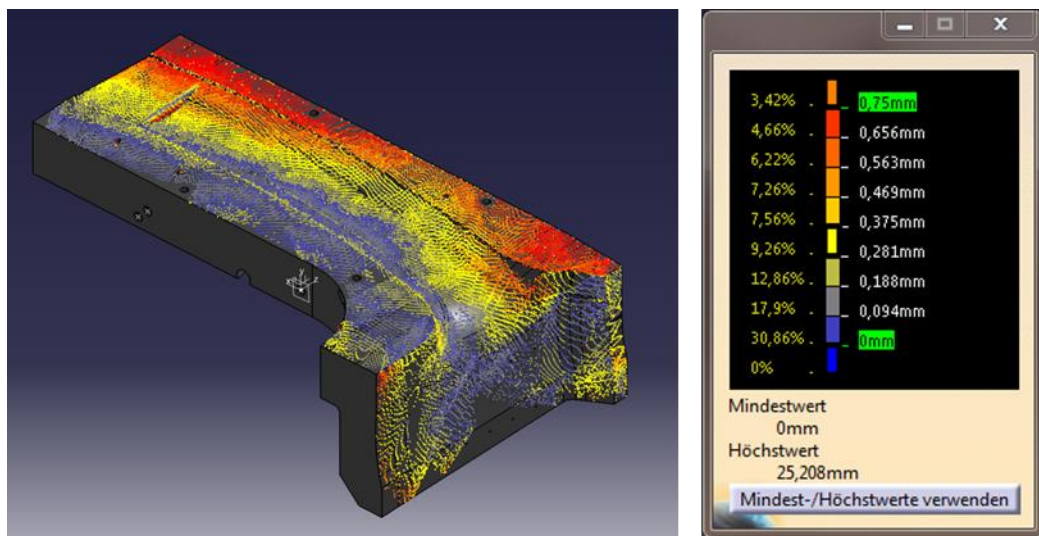


Figure 3: Distance analysis of the large-area tooling normal to the CAD-Surface

A difference between the left and the right side of the mold is noticeable, which can be explained by the distance towards the reference origin and a resulting error in orientation.

The analysis after ten heating cycles shows similar results over most parts of the tooling. However there are signs of abrasion in the area of the bend that have been caused by a collision during the automated preforming process.

For the edge-tooling the 90 % of the measured points have a deviation of 0.3 mm or less. The narrow edge area is the most accurate to size. In Figure 4 you can see that the area of the largest deviation is at the transition of the edge. The deviation at this point is roughly 0.56 mm.

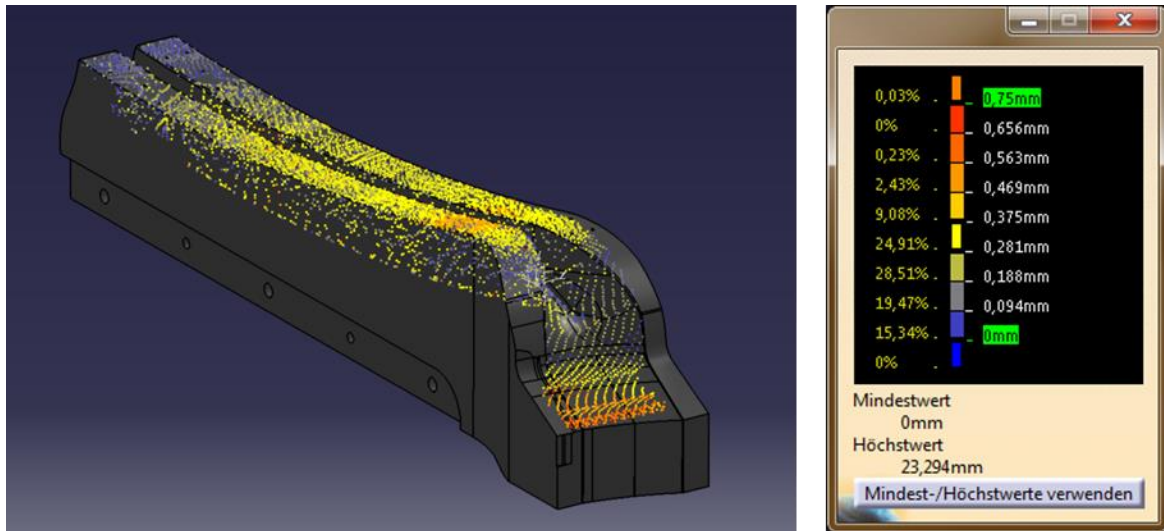


Figure 4: Distance analysis of the edge-tooling normal to the CAD-Surface

For the sake of draping, matching male geometries were produced in the same SLS process. These stamps match the molds geometry and are sufficiently accurate for the draping.

4.2 Test of integrated Functionalities

One of the key assets of rapid tooling for our use case is the integration of heating and fixation into the molds design. In the following a short description of two tests is given that were conducted in order to validate the suitability for preforming.

4.2.1 Methodology

In the first test the two molds were setup in an air conditioned room with 21.6 °C and 50.8 % humidity. Thermocouples were placed inside the molds and on their surface. The placement of the thermocouples is depicted in Figure 5. In addition to the depicted placements there is one extra thermocouple per tooling that is placed right next to the heat cable to observe possible heat accumulations. The heating cables were then activated and the temperature profile taken by the thermocouples was recorded. Additionally the heating was documented with a thermographic camera. The camera used had a resolution of 640 × 512 pixels and during heating pictures were taken every ten seconds. When the binder activation temperature of 80 °C was reached throughout the surface the heating was stopped. Subsequently compressed air was led through the pneumatic orifices for cooling. The molds were not covered during the test.

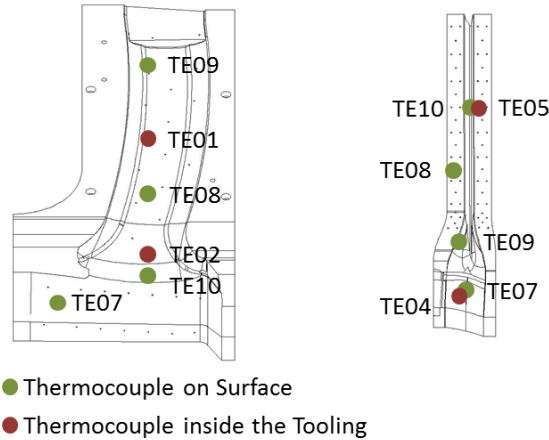


Figure 5: Schematic of the thermocouples position during heating

The functionality of the integrated pneumatic fixation was validated in a second test. Four wrought materials with different material properties were chosen. Differences in the materials regarded weight, air permeability, thickness, weave and material itself. The materials were cut into rectangular pieces with a size to cover up the orifices on the flat part of the large-area tooling. This was done because the draped or bend material is already held in place and therefore a validation of the pneumatic fixation is difficult. All orifices that were not covered by material were sealed with tape to prevent air leakage. The four materials are shown in Figure 6. Corresponding material properties can be found in Table 2.

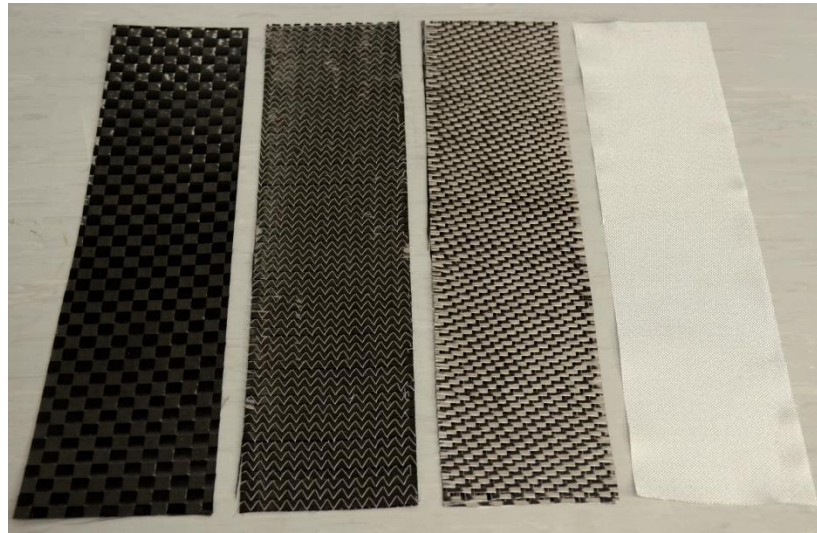


Figure 6: The four materials used for the test of the pneumatic fixation from stiff (left) to loose (right)

Table 2: Material Properties of the Textiles

Manufacturer	Fiber	Weave	Areal Density [g/m²]
Hexcel	Carbon Fiber	Spread Tow Plain Fabric	220
Saertex	Carbon Fiber	NCF biaxial 0/90	262
Cytec	Carbon Fiber	Satin Fabric	370
PI-Interglas	Fiberglass	Cross Twill	3.13

The cut-pieces were placed on the large-area tooling and pneumatically fixed. Afterwards the tooling was tilted to 45° and 90°. The same vacuum pump was used for all cut-pieces and the volume flow rate for each cut-piece was recorded.

4.2.2 Results Heating-/Coolingrate

The chosen heating principle is inherently slow. Even the thermocouples next to the heating cables take twelve minutes to reach 80 °C. Because of the self-regulatory properties of the heating cables the heating rate decreases with rising temperature. Figure 7 shows the temperature graph over time for the large-area tooling. All thermocouples except for TE03 which is next to the heat cable show a delayed increase in temperature. However after the first delay all the thermocouples show a similar slope with an exception of TE09 which malfunctioned after 13 minutes. TE02, which is one of the inner sensors, reaches 80°C after 27 minutes. The second inner sensor reaches 80 °C after 30 minutes. The superficial sensors take roughly 35 minutes to reach 80 °C. The heating rate is 1.57 to 2 °C/min. Because of the heat loss at the surface the heating rate declines at higher temperatures. Also the power is not sufficient to reach the maximum temperature of the heating cables of 120 °C. All sensors show a similar temperature progression during cooling. The cooling rate is roughly 5.5 °C/min.

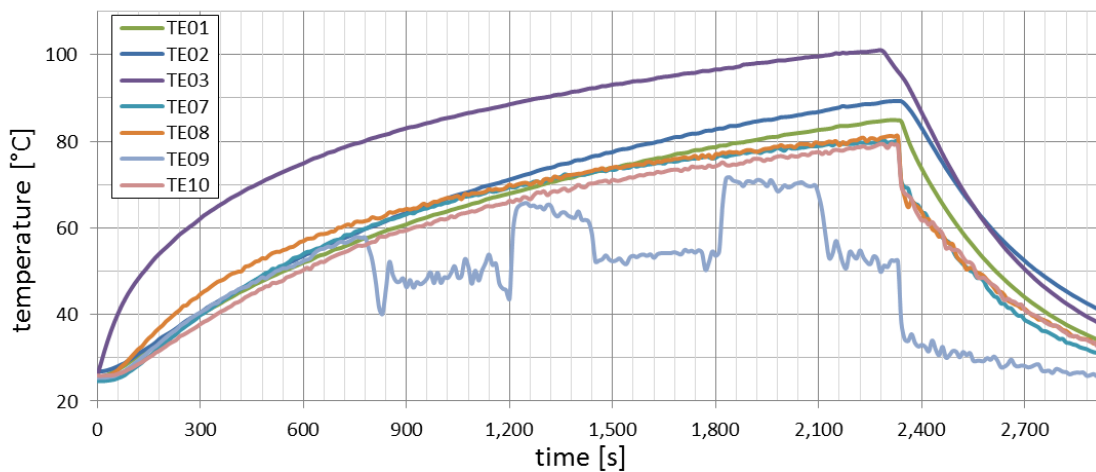


Figure 7: Temperature graph over time during heating and active cooling of the large-area tooling

In comparison the heating rate of the edge-tooling is higher. In Figure 8 we see a steep incline of two temperature graphs, i.e. TE06 and TE10, with a heating rate of 13.4 °C/min. TE06 reaches 80 °C after 5.3 minutes and TE10 after 6.2 minutes respectively. The fast heating of TE10 can be explained with its position between the edges of the tool where the heat is accumulated. Therefore the inner sensors show a deviation of almost 15 °C for TE05 and 5° for TE04. The other superficial sensors do not reach a sufficient temperature. Their position is not close enough to one of the heat cables.

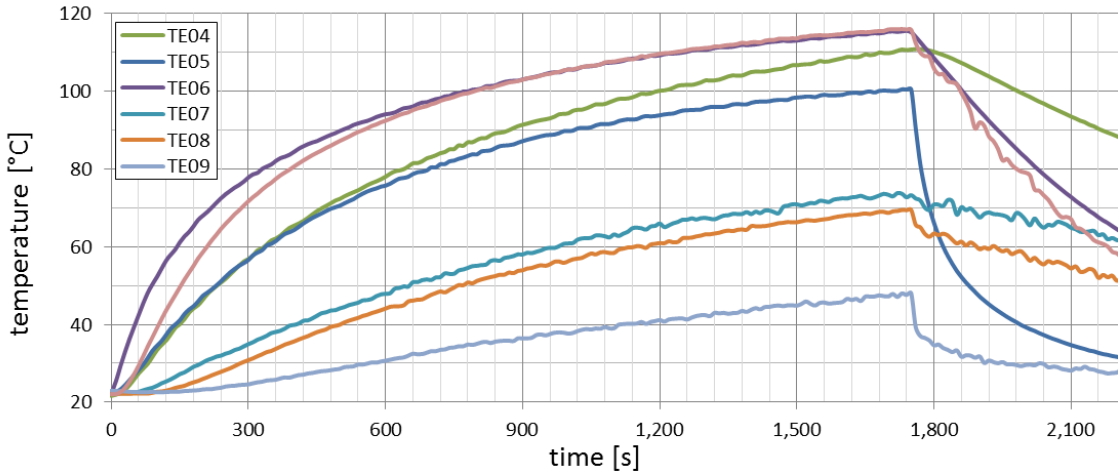


Figure 8: Temperature graph over time during heating and active cooling of the edge-tooling

The cooling rate between the sensors varies noticeably. This is due to the fact that the orifices that are used for air cooling are not distributed equally over the whole surface. Sensors like TE05 that are in close proximity to the cooled area of the mold have a significantly higher cooling rate of roughly 20 °C/min.

4.2.3 Results Heat distribution

Apart from the heating rate an equal distribution of heat over the surface is important. Figure 9 shows a series of thermographic pictures of the large-area tooling after 5, 10, 27 and 35 minutes.

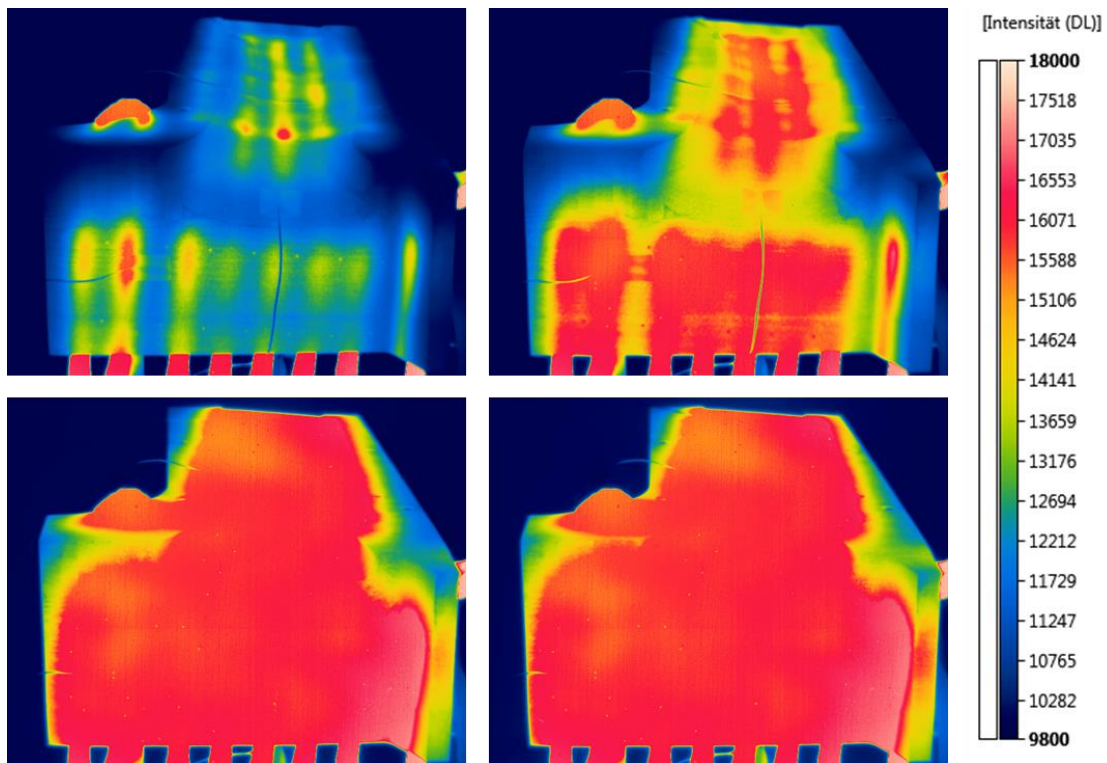


Figure 9: Heating of the large-area tooling after 5, 10, 27 and 35 minutes

After 5 minutes the superficial sensors indicate a temperature between 37.8 °C and 44.7 °C. The thermography shows hotspots of roughly 62 °C on the left side and in the center of the mold after 5 minutes. Therefore the distribution is not consistent in the beginning. After ten minutes the heat is already distributed more evenly. However areas that are not close to the heating cables still show a temperature difference of over 25 °C (Figure 7). The first sensor reaches the desired temperature of 80 °C after 27 minutes. At this point the temperature difference shown by the other sensors is roughly 5 °C. The thermographic picture at that time shows that the heat is evenly distributed over the formative surface. At the edges of the surface cooler spots remain. That does not significantly change after 35 minutes when all sensors have reached 80 °C. The active cooling of the large area-tooling with air decreases the cooldown time to 40 °C significantly, from over 30 to roughly 5 minutes. The temperature distribution over the surface is uneven during cooling. This is primarily caused by the fast cooling areas surrounding an orifice and a low thermoconductivity of the material. This is shown in a series of thermographic images in Figure 10. The images were taken after 1, 2, 3 and 5 minutes. After 5 minutes a large portion of the surface is back to 40 °C or less. At this temperature an activated preform can potentially be demolded. However there is still an area on the left side of the formative surface which has a temperature over 50 °C. Therefore a more consistent placement of the orifices is needed if an even cooling of the surface is desired.

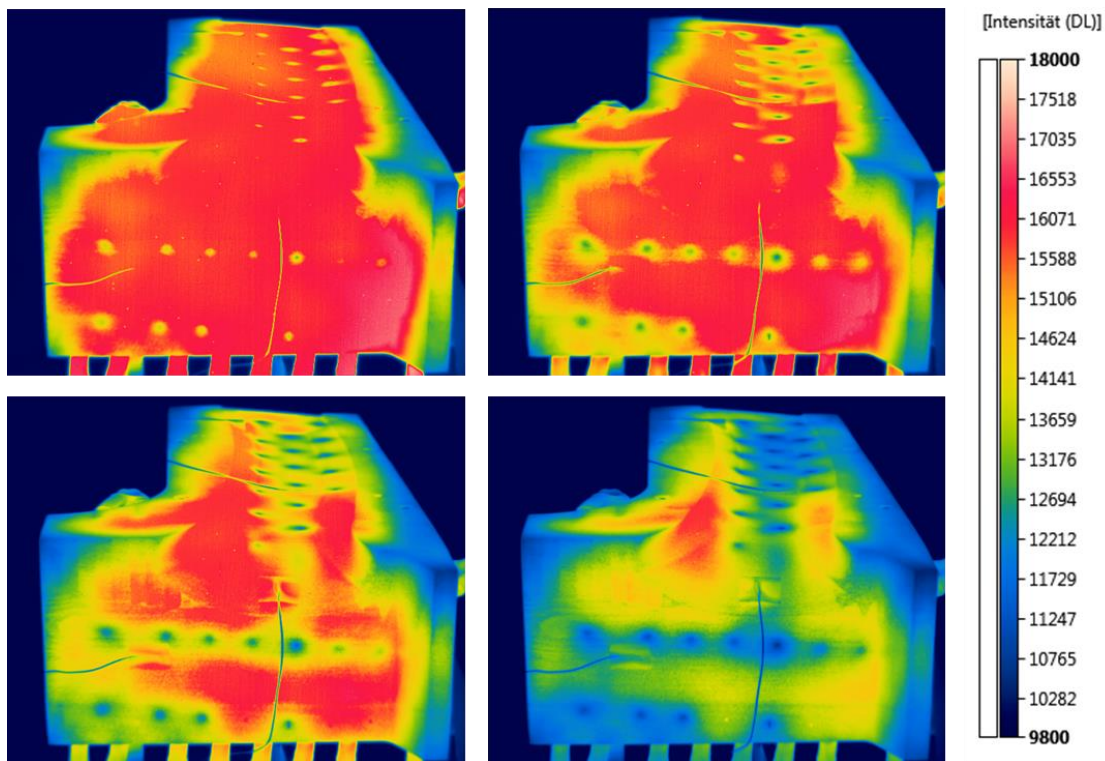


Figure 10: Cooling of the large-area tooling with air after 1, 2, 3 and 5 minutes

The heat distribution on the surface of the edge-tooling is inconsistent. Formative areas of the surface are still at 30 °C whereas the activation temperature is reached in other areas of the surface. This can be seen on the left part of Figure 11 that shows the edge-tooling after 4 minutes of heating. Although the tooling is completely heated after 28 minutes (Figure 11 center) the irregular temperature is not suitable for the activation of the binder. Finally the cooling shows

similar results because the heat is accumulated in the narrow edge where no orifices for airflow are placed.

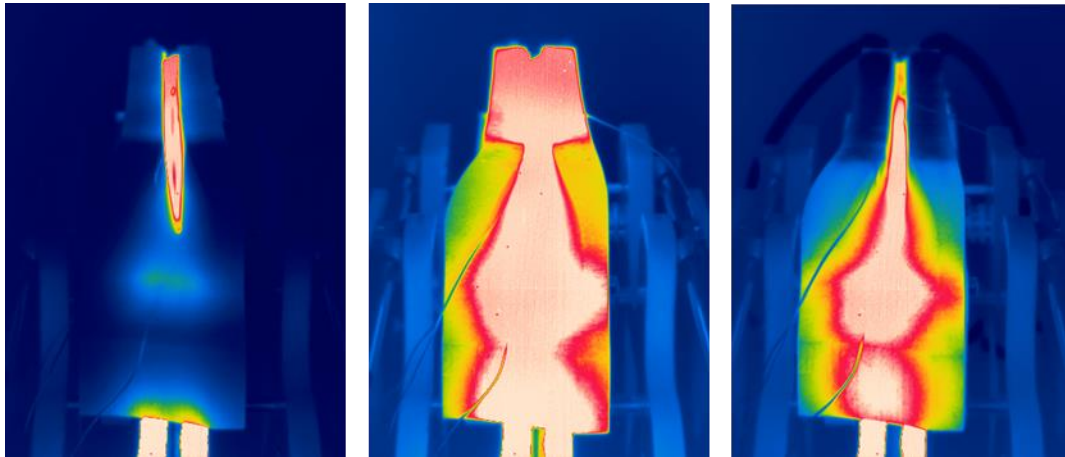


Figure 11: Heating and cooling of the edge-tooling

4.2.4 Results ply fixation

The test of the ply fixation shows that the inner vacuum chamber and the orifices are sufficient to hold the four different textiles. The cut-piece stays in the desired place without shifting. The volume of air varies depending on the permeability of the material. This does not affect the fixation. Figure 12 shows the experiment in 90° inclination with two materials – the Hexcel carbon fiber spread tow plain fabric and PI-Interglas fiberglass cross twill.

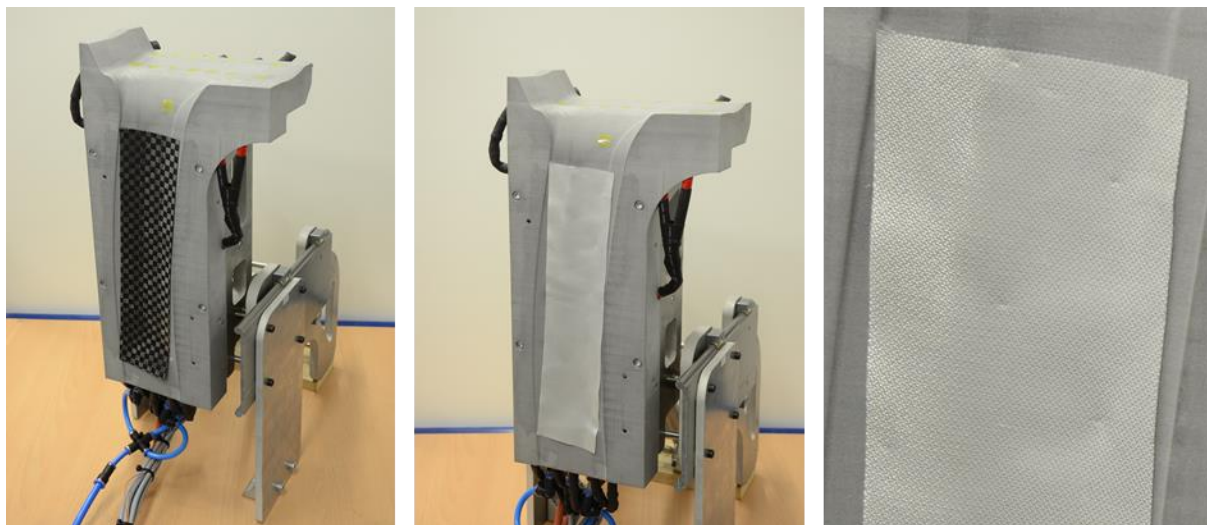


Figure 12: Test of the ply fixation with different textiles

The detail on the right shows that fine materials like the fiberglass twill can get sucked into the orifices, resulting in a damaged textile. It is not possible to manufacture smaller channels with the SLS process due to the risk of clogging by the unsintered material. Therefore this kind of fixation is applicable for stiffer materials only. This problem was not observed with the other materials.

4.3 Application of the molds in use case

The shown concept of function-integrated molds was tested on an example component to estimate the application potential. For mapping an industry-related process, e.g. preforming for RTM manufactured components, an automated preforming process was developed and implemented in a test rig. We hereby automated the handling of the ply stacks, the draping into the molds, the assembly of the sub-preforms and the final activation of the binder. In order to capture the properties of the molds as comprehensively as possible, a component was selected that requires a multi-stage preforming process. The component is made up of four sub-preforms, which are assembled sequentially by two large-area toolings and afterwards by two edge toolings. For the draping of the sub-preforms, a stamp forming process was chosen. The stamps represent the corresponding male counterpart of the female molds and were also made of PA12 enriched with aluminum powder using the same SLS process used for the molds. This made it possible to investigate the application of the presented concept for corresponding surfaces. Due to the complex geometry the stamps were partly kinematized. After draping, the sub preforms were fixated through integrated orifices as shown in Figure 12. We successfully assembled and activated four sub-preforms into one final preform with the use of the discussed molds. The pneumatic system adequately held the ply stack in place during rotation and assembly. Also the mold material allowed a good thermal distribution and enough temperature resistance for the binder to be activated. The graphs in Figures 7 and 8 show the thermal progression of the molds in open state. For the large-area tooling approximately 40 minutes and for the edge tooling approximately 30 minutes are required in order to reach the binder activation temperature of 80 °C. When the tooling is in closed state the open area for thermal radiation is reduced and therefore heat congestion reduces the required time to reach 80 °C to approx. 5 minutes (Figure 13). As soon as the binder activation temperature is reached the heat supply can be stopped since the temperature overshoots due to thermal conductivity. The cooling rate of 1.1 °C/min was comparably low in the closed state and the cooldown took over 40 minutes. After cooling down the demolding was executed without adherence between the mold and preform. Possible improvements in order to increase the cooling rate are additional enlarged orifices in combination with an increased volume flow rate.

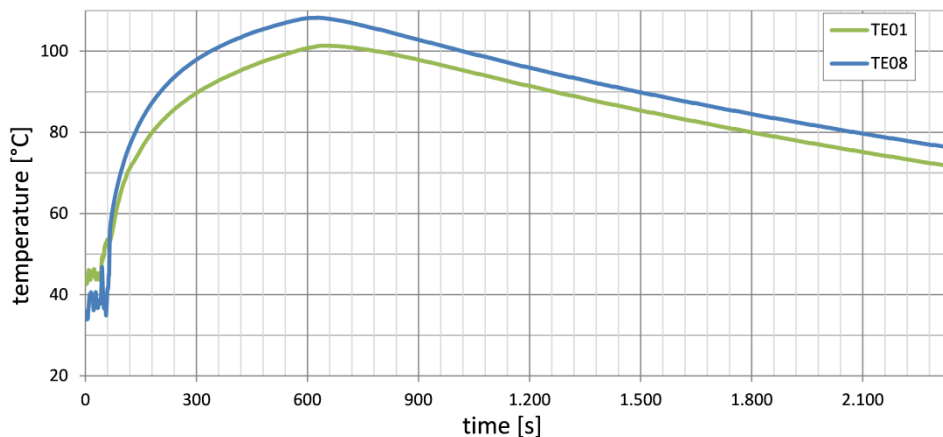


Figure 13: Temperature graph over time during heating of large-area tooling in closed state

5. DISCUSSION OF RESULTS

The geometric analysis shows that the accuracy of the toolings is sufficient for preforming. Major geometric deficiencies caused by thermal warping could not be detected. However the referencing of the molds can be problematic if markers are printed. This is because of shrinking which affects the position of reference markers. In our case the large-area mold shrunk by 0.24 mm in length, relative to the central reference point. This may cause inaccuracies in an automated process where an accurate knowledge of the molds position is essential. Therefore the printed referencing points need an improved design that compensates occurring inaccuracies. The geometry was stable over multiple heating cycles and despite the mechanical loads during the application in an automated preforming process. However the number of heating cycles was relatively low. A final assertion of the long-term durability cannot be made. In addition to the outer geometries the production of the inner design works well and the resulting surface quality is sufficient for draping without damaging the textiles.

Although the heating rate is low at under 2 °C/min, the principle of heating with self-limiting heating cables is feasible. The desired temperature can be reached and the resulting temperature distribution is sufficiently homogenous for the activation of a binder. Also we determined the heating rate with uncovered molds that loose heat to ambient rapidly. The use case application shows that higher heating rates are possible. In the closed mold 80 °C were reached after 5 minutes. We also saw that the thermal conduction is not sufficient to heat parts of the mold that are distant to the source. This can be avoided with a design that keeps the heating source close to the surfaces that needs to be heated. The limitation for design is the flexibility of the heating cables. Further the active cooling with pressurized air works well. The cooldown time was significantly reduced.

Another feature we tested is the integration of channels for sensors that measure just beneath the surface. The results we saw were ambiguous. In one case the sensors showed excellent results that matched the temperature of the thermocouples applied onto the surface. In this case the integration of the sensor placement in the initial design is an elegant solution to get accurate results for an inline process monitoring. However for the second tooling the results were not accurate. This might be due to a clogged channel or a flawed contact between the sensor in the narrow channel and the surface that should have been measured. The general principle works – the design requires changes.

Finally the fixation of the plies during draping and merging of the sub-preforms was investigated. The holding force is sufficient for a variety of different materials. Additionally the plies can be held in place during draping in order to ensure accurate positioning of the draped plies. The fixation has great potential for a variety of applications especially in an automated process when fixation is needed during handling operations. In conclusion the presented results show that the additively manufactured toolings made from alumide have potential for the application in preforming, even though the design needs to be improved in its details.

6. CONCLUSIONS

The flexibility of additive manufacturing allows the integration of complex inner geometries in the design. The functions we thereby enabled worked within the specifications for our use case. Especially the heating with self-limiting heat cables and the fixation through an integrated vacuum chamber turned out to be effective. Potential improvements regarding the design were identified and can be applied to future works. PA12 enriched with aluminum is a suitable

material for preforming molds if the infusion and curing of the part is done in a separate process. This is especially useful for an automated CFRP production with multiple sub-preforms. The potential cost savings that we saw by comparing the most economical quote we received for a standard aluminum mold without additional functions and the price of the additively manufactured toolings discussed was 660%. Further the corresponding male geometries were included in the price which makes the cost difference more significant. Therefore rapid tooling is an economic alternative for the production of complex CFRP preforms, especially for small batch series.

7. REFERENCES

- [1] M.A. Leon-Cabezas. Innovative advances in additive manufactured moulds for short plastic injection series. *Procedia Manufacturing*, 2017.
- [2] J. Sloan. Additivemanufacturing.media: 3-d printing autoclavable composite molds <https://www.additivemanufacturing.media/blog/post/3-d-printing-autoclavable-composite-molds>, 05 2016.
- [3] S.Black. Additivemanufacturing.media: Using 3d printing for composite molds and tools: The trend continues [https://www.additivemanufacturing.media/blog/post/using-3d-printing-for-composite-molds-and-tools-the-trend-continues-\(2\)](https://www.additivemanufacturing.media/blog/post/using-3d-printing-for-composite-molds-and-tools-the-trend-continues-(2)), 06 2016.
- [4] M. Fette. Optimized and cost-efficient compression molds manufactured by selective laser melting for the production of thermoset fiber reinforced plastic aircraft components. In *15th Machining Innovations Conference for Aerospace Industry*, 2015.
- [5] T. Z. Sudbury. An assessment of additive manufactured molds for hand-laid fiber reinforced composites. In *The International Journal of Advanced Manufacturing Technology*, Bd. 90,, number 5-8, pages 1659–1664, 2017.
- [6] H. Lengsfeld. *Faserverbundwerkstoffe - Prepregs und ihre Verarbeitung*. Hanser, 2015.
- [7] A. Buchheim. Drape-forming methods for the automated preforming of composite helicopter structures. *Sampe*, 2017.
- [8] H. Fabrics. Product data e01 powder, 2003.
- [9] EOS. Eos - materialdaten <https://eos.materialdatacenter.com/eo/>.